Synthesis and Characterization of Polyfurfural Nanoparticle

Ahmad Al-Hamdan[1], Ahmad Al-Falah[1,2], Fawaz Al-Deri[1],
Ali Alasmi[3], Joumaa Merza[3,4], Mirna Jabbour[5], and Waed Abodaboos[5]

[1]*Department of Chemistry,*
 Damascus University,
 Damascus, Syria
[2]*Faculty of Pharmacy,*
 Arab International University (AIU),
 Damascus, Syria
[3]*Department of Chemistry,*
 Albaath University,
 Homs, Syria
[4]*Faculty of Dentist,*
 Arab Private University for Science and Technology,
 Homs, Syria
[5]*Faculty of Pharmacy,*
 Damascus University,
 Damascus, Syria

In this paper, polyfurfural is synthesized by hydrochloric acid as catalyst in ethanol. The resulting polymer is characterized by FT/IR, EDS and XPS to determine the polymer structure. By SEM, the morphology of resulting polymer is studied. As found, the polymer consists of globule particles, which clump together and form clusters with average size of about 700 nm. Globule particles are composed of small spherical particles with an average size of 18.6 nm. Polymer thin film is fabricated by anchoring on glass; thin film has rough surface ($Rms = 2.12 \pm 0.3$ nm) and nanoparticles size of 17.8 nm. Based on x-ray diffraction, the crystallization ratio and the nanocrystals' size (7.42 nm) are calculated. A new method for the determining nanoparticle size from x-ray diffraction data is proposed. The particle size is of 16.18 nm that is less than the size specified by SEM or AFM.

У даній роботі поліфурфурол синтезується соляною кислотою як каталізатором в етанолі. Одержаний полімер характеризується інфрачервоною спектроскопією на основі перетвору Фур'є, енергодисперсійною рентґенівською спектроскопією та рентґенівською фотоелектронною

спектроскопією для визначення структури полімеру. Сканувальною електронною мікроскопією вивчається морфологія одержуваного полімеру. Як виявилося, полімер складається з частинок ґлобули, які злипаються в купу й утворюють скупчення із середнім розміром близько 700 нм. Частинки ґлобул складаються з дрібних сферичних частинок із середнім розміром у 18,6 нм. Полімерна тонка плівка виготовляється шляхом прикріплення на склі; тонка плівка має шерстку поверхню (із середнім квадратичним значенням відхилень висоти профілю від середньої лінії $Rms = 2,12 \pm 0,3$ нм) і наночастинки розміром у 17,8 нм. На основі дифракції рентґенівського випромінення розраховуються коефіцієнт кристалізації та розмір нанокристалів (7,42 нм). Запропоновано новий метод визначення розміру наночастинок за даними дифракції рентґенівського випромінення. Розмір частинок становить 16,18 нм, що менше розміру, визначеного сканувальною електронною мікроскопією або атомно-силовою мікроскопією.

1. INTRODUCTION

Conducting polymers play an important role in the field of material science because of their excellent electrical, optical, optoelectronic properties [1], ease of fabrication, flexibility, and chemical inertness [2]. Although conducting polymers were discovered only seventy years ago, but they have a wide range of applications [3]. Conducting polymers are used in gas-separation membranes [4], membranes [5], optical displays [6], solar cells [7], rechargeable batteries [8], sensors, biosensors [9], light-emitting diodes [10], and electrochromic devices [11]. Polypyrrole, polyfuran, polythiophene and their derivatives are common conducting polymers [12]. Polymers can be synthesized by chemical, electrochemical, or plasma methods [1]. Furfural was polymerized by electropolymerization [13, 14], and plasma methods [15]. It was used for fabrication of film-modified electrodes [14, 15]. It is also known that dipping these films with other materials, such as iodine, acid, or others, modifies the electrical and optical properties [1]. Similar monomers synthesized by chemical polymerization, such as 2-carboy aldehyde thiophene, were polymerized by acid (RSO$_3$H) [16]. The polymerization took place on the expense of the aldehyde group by the electrophilic addition mechanism. The polymer was reduced by hydrazine to ob-

tain the final product [16].

In this research, we synthesize polyfurfural by chemical polymerization by acid catalysis in ethanol. Characterization is made by FT/IR, XPS, and EDS. Nanoparticle size of polymer is studied by SEM, AFM, and XRD.

2. EXPERIMENTAL

2.1. Materials and Measurements

There are used furfural 99% sigma, hydrochloric 35.5% acid sigma, ethanol 98% sigma.

Polyfurfural was characterized with UV spectrophotometer between 380–800 nm by Optizen model OUV322 and FT/IR (JASCO FT/IR model M4100) spectrophotometer between 4000 and 400 cm^{-1} by KBr disk.

Surface morphologies were checked by SEM, EDS and XPS (TESCAN model MIRA3). Polymer film was checked by AFM (Nanosurf model eseyscan2); polymer powder film was checked by XRD (Philips, model: PW1370, Cu (0.154056 nm) step size of 0.05 deg.).

2.2. Synthesis

Furfural (21 mmole, 2.0 g) was dissolved in ethanol (25 ml), and then hydrochloric acid 35.5% (10 ml) was added. Mixture solution was placed at room temperature for 8 h. Colour of reaction solution changed to red and then purple. Later on, a black product was precipitated. The polymer forms a thin film on the surface of the reaction vessel or any substrate within the reaction solution. The precipitate was filtered and washed with NaOH (15%) solution, ionized water and ethanol several times, then, dried at 105°C for 48 hours. It was kept for later study.

3. RESULTS AND DISCUSSION

Polyfurfural is a black powder, insoluble in common organic solvents, such as ethanol, methanol, THF, ethyl acetate and acetonitrile, partially soluble in acetone, well soluble in formic acid, DMSO and DMF. It melts at > 300°C and then decomposes.

3.1. UV−Vis Spectra

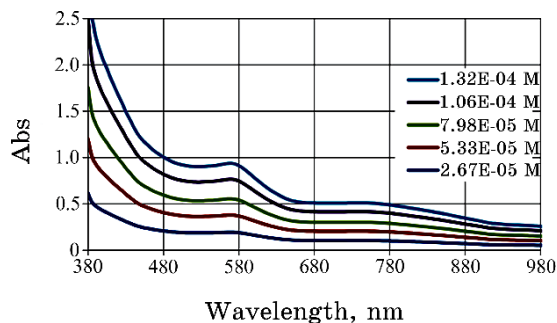Reaction solution contains furfural of different concentration

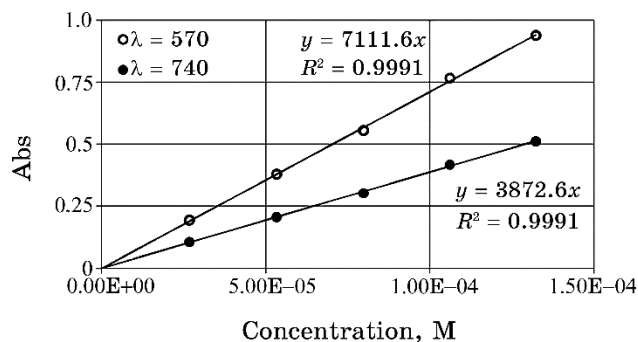**Fig. 1.** UV−Vis spectra of reaction mixture solutions.

Fig. 2. Absorption (at maximum absorption peak) *vs* concentration.

$(2.67 \cdot 10^{-5}$ M, $5.33 \cdot 10^{-5}$ M, $7.89 \cdot 10^{-5}$ M, $10.60 \cdot 10^{-5}$ M, $13.21 \cdot 10^{-5}$ M) and hydrochloric acid of 3 M in ethanol. These solutions were kept at room temperature for 24 hours.

Then, the UV−Vis spectrum was recorded on the blank of ethanol and acid (3 M). Figure 1 shows the UV−Vis spectra. Absorption spectrums show two maximum absorption peaks at 570 and 740 nm.

Figure 2 shows absorption (at maximum absorption peaks) *vs*. concentration of furfural. Values of molecular absorption coefficient are of 3872 and 7111 l/(mole·cm), respectively. Good stability of absorption at two different peaks is indicative of light absorption by a single component.

3.2. FT/IR Spectrophotometer

FT/IR spectrums of monomer and polymer were recorded (Fig. 3). For monomer in Fig. 3, *a*, absorption band at 3130 cm^{-1} was due to aromatic C−H, peaks about 2845 and 2812 cm^{-1} are attributed to the C−H aldehyde, peak at 1670 cm^{-1} was related to C=O aldehyde,
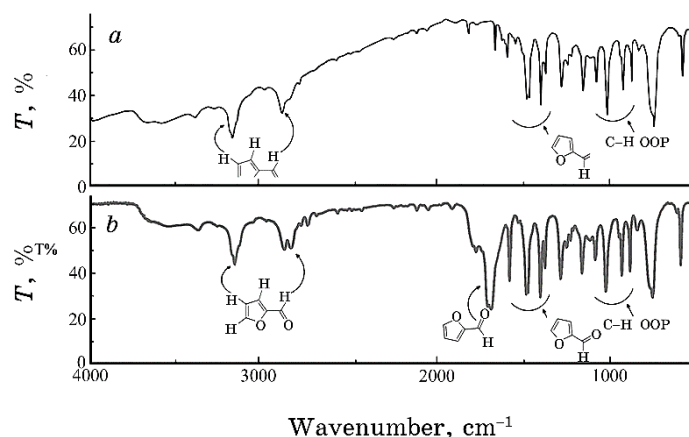
Fig. 3. FT/IR spectrum of monomer (*a*) and polymer (*b*).

and the peaks between 1500 cm^{-1} and 1000 cm^{-1} were due to C=C in furan ring and C–H out of plane [17]. In Figure 3, *b*, FT/IR spectra of polymer have same peaks as in the spectra of monomer, but peak at 1670 cm^{-1} (C=O aldehyde) is weakened due to consumption of aldehyde by polymerization. No significant difference was observed between the spectrum of furfural and its polymer.

According to above findings and references, the following formula for polymer can be suggested:

PFF

poly(EDOT — methine)
(Zaman et al. 2005) .
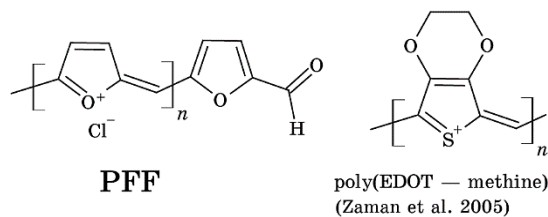
3.3. Elemental Analysis by EDS Analysis

The EDS technique utilizes x-rays, which are emitted from the sample during bombardment by the electron beam, to characterize the elemental composition of the analysed volume on a micro- or nanoscale. An electron beam is scanned across the sample surface and generates x-ray fluorescence from the atoms in its path. The energies of the x-ray photons are characteristic of the element, which produces them. The EDS x-ray detector measures the number of emitted x-rays *vs.* their energy. The energy of the x-ray is characteristic of the chemical element, from which the x-ray is emitted [18].

Table 1 shows EDS results for three areas of polymer surface. A

TABLE 1. EDS analysis for three areas of polymer surface.

Element	Area 3		Area 2		Area 1		average	Ele/C
	at.%	wt.%	at.%	wt.%	at.%	wt.%		
C	67.6	50.9	66.1	49.7	65.6	49.4	66.4	100.0
O	18.9	19.0	20.7	20.8	21.3	21.3	20.3	30.6
Cl	13.5	30.1	13.2	29.4	13.1	29.2	13.3	20.0
Total	100.0	100.0	100.0	100.0	100.0	100.0	100.0	100.0

slight difference is noted due to the inaccuracy of the EDS analysis in determining the ratio of elements. The polymer contains carbon 66.4%, chlorine 13.3%, and oxygen 20.3%. The Cl/C ratio is of about 20% (one chlorine atom *per* five carbon atoms), and the O/C ratio is of about 30.6%; higher percentage of oxygen is due to water molecules adsorbed in the polymer structure.

3.4. Scanning Electron Microscope (SEM)

The morphological features of polyfurfural synthesis have revealed that growth mostly occurs in the globular form with some changes due to solvent effects.

Typical SEM images of polyfurfural preparations are shown in Fig. 4. The photographs show a globular structure clumped together as clusters. Figure 4, *a*, *b* shows the average size of globules of about 700 nm. The globule particles were composed of small spherical particles with an average size of 18.6 nm (Fig. 4, *c*). Polymers grow to be spherical particles and then begin to clump on each other to form huge globules (tens of times bigger). Globule particles were merged together to be clustered.
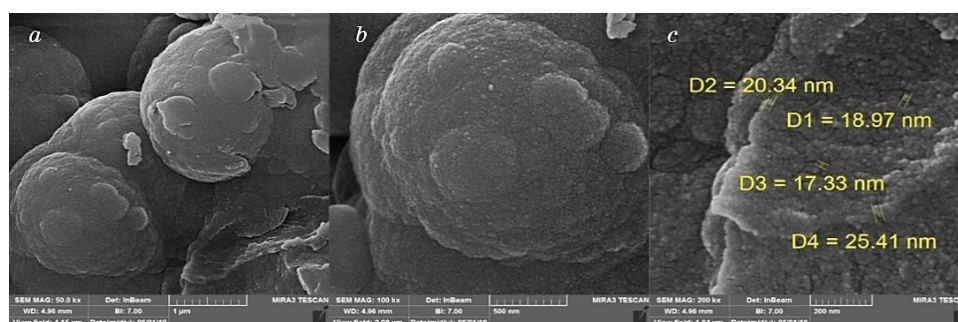

Fig. 4. Images obtained by means of the scanning electron microscope for polyfurfural.

3.5. X-Ray Photoelectron Spectroscopy Analysis

The sample is subjected to irradiation from a high-energy source. The x-ray penetrates only 1−10 nm under the surface (depending on the tilting angle of sample). As an atom absorbs x-rays, the energy will produce electron from C $1s$ orbital. The ejected electron has a kinetic energy that is related to the energy of the incident beam, and the electron binding energy is specific for the element [19].

Figure 5 shows x-ray photoelectron spectroscopy for polymer (PFFu). The spectra have peaks: first one at 536.1 eV (O $1s$), second one at 287.8 eV (C $1s$). With an analysis of (C $1s$) spectra (Fig. 6), it is possible to determine how much carbon is bound to the hydrogen and oxygen in the polymer structure as follows:
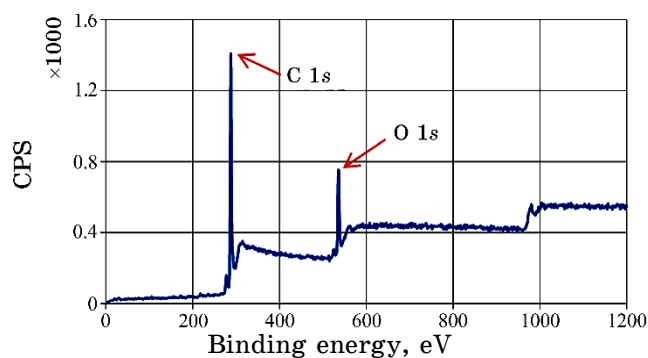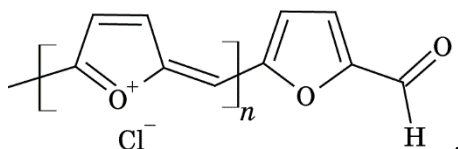

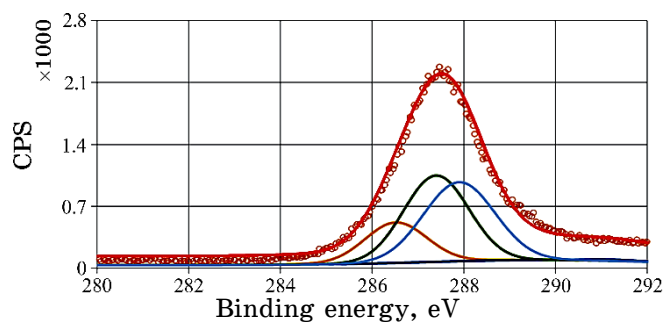**Fig. 5.** X-ray photoelectron spectroscopy for (PFFu).

Fig. 6. (C $1s$) XPS spectra with typical peaks.

TABLE 2. Comparison between the types of carbon in polymer structure by XPS.

No.	Name	Bond energy, eV	FWHM, eV	Area	Area%
1	C–H (ring)	287.9	1.86	56986.4	40.64%
2	C–H	286.5	1.86	25835.6	18.43%
3	C–O	287.9	1.86	56779.2	40.50%
4	C=O	291.2	1.86	609.456	0.43%

Table 2 shows comparison between the types of carbon in polymer structure:

1. C–C*(H)–C: carbon atom bonded to carbon and hydrogen in the furan ring at 287.9 eV (area = 40.64%);

2. C–C*(H)–C: carbon atom bonded to carbon and hydrogen out of furfural ring at 286.5 eV (area = 18.43%);

3. C–C*–O: carbon atom bonded to carbon and oxygen in the furan ring at 287.9 eV (area = 40.5%);

4. C–C*=O: carbon atom bonded to carbon and oxygen in aldehyde group at 291.2 eV (area = 0.43%).

3.6. Atomic Force Microscopy (AFM)

Thin film of PFFu was fabricated by anchoring in the reaction mixture [20]. The resulting films were studied by atomic force microscopy (AFM). Figure 7 shows topography and 3D image of polymer film. AFM was used as a powerful technique to study the morphology of thin-films' surfaces and to determine the nanoparticle size. The measurement includes scans of 2 μm×2 μm areas of thin film. The nanoparticle size was of about 17.8 nm. Film consists of asym-
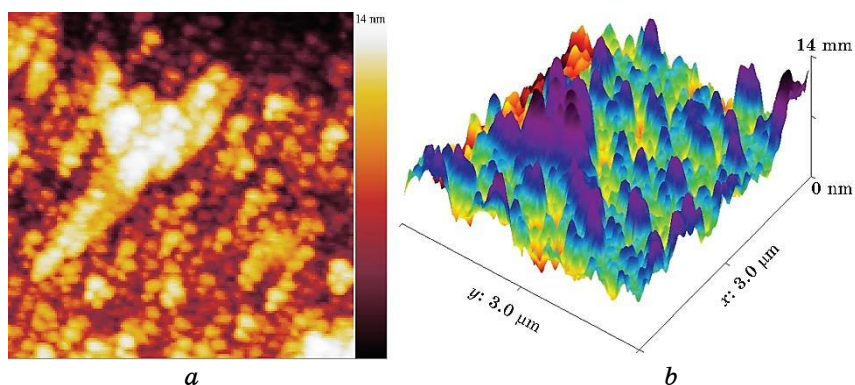

Fig. 7. Topography (*a*) and 3D image (*b*) for PFFu film.

metric particles, which form a rough surface ($Rms = 2.12 \pm 0.3$ nm and $R_a = 1.67 \pm 0.3$ nm).

3.7. X-Ray Diffraction (XRD)

X-ray diffraction data are commonly used to determine the crystalline percentage and crystal size. The size of the crystals is calculated from the Scherrer's equation, and crystalline percentage is given by Eq. (1):

$$P_{cry}\% = \frac{A_{cry}}{A_{cry} + A_{amo}} \cdot 100 \,, \tag{1}$$

where A_{cry} is a sum of crystalline peak areas (sharp peaks) and A_{amo} is an area of amorphous peak [21].

Figure 8 shows the analysis of x-ray diffraction data. The crystalline percentage $P_{cry}\%$ was of about 9.63%.

Table 3 shows crystal size, percentage areas of crystalline peaks and their parameters; crystal size is of 7.42 nm.

Semi-crystalline nanoparticles are formed in three stages: nucleation, crystal growth, and then, an amorphous shell formed around the small crystals. Sometimes, these particles agglomerate to form larger particles or clusters. The percentage of the crystalline part represents the mass percentage, which is given by Eq. (2):
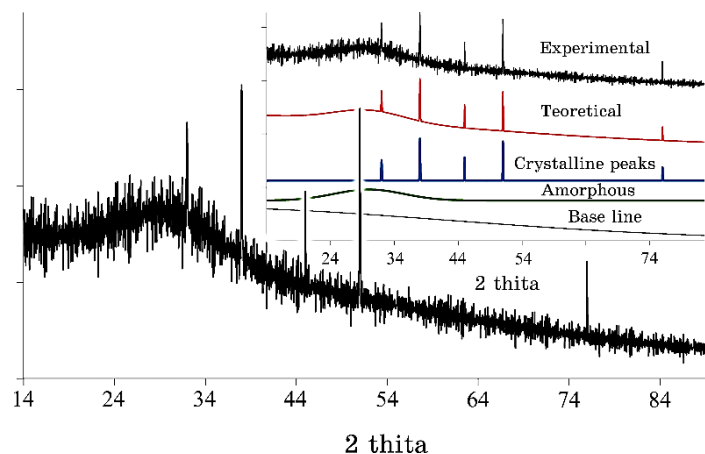
$$P_{cry}\% = \frac{m_{cry}}{m_{tot}} \cdot 100 \,, \tag{2}$$

Fig. 8. X-ray diffraction (XRD) for polymer.

TABLE 3. Percentage areas of crystalline peaks and their parameters.

Crystal size, nm	P, %		Size, nm	Theta, rad	W.H.T., rad·10^{-2}	Area	Peak
		3.43%	6.12	0.3314	2.40	433.56	P1
		1.11%	10.60	0.3925	1.42	140.92	P2
7.42	9.63%	0.72%	11.03	0.6629	1.59	91.40	P3
		1.75%	5.79	0.2791	2.49	221.56	P4
		2.61%	7.85	0.4448	1.96	329.71	P5
	90.37%			—		11421.37	amorphous

where m_{tot} is mass of particles and m_{cry} is mass of the crystal.

Nanoparticles are spherical; their mass can be calculated by Eq. (3):

$$m_i = d_i \frac{4\pi}{3} r^3 . \tag{3}$$

Let us substitute Eq. (3) into Eq. (2):

$$P_{cry} \% = \frac{d_{cry} \frac{4\pi}{3} r^3_{cry}}{d_{av} \frac{4\pi}{3} r^3_{tot}} \cdot 100 . \tag{4}$$

With an acceptable approximation, the density can be considered constant, and Eq. (4) can be written as:

$$P_{cry} \% = \frac{r^3_{cry}}{r^3_{tot}} \cdot 100 , \tag{5}$$

$$P_{cry} \% = \frac{D^3_{cry}}{D^3_{tot}} \cdot 100 , \tag{6}$$

where D_{cry} is nanocrystal size (by Scherrer's equation), and D_{tot}—nanoparticle size:

$$D_{tot} = \frac{D_{cry}}{\sqrt[3]{P_{cry}}} . \tag{7}$$

This equation gives the volume of the nanocrystals with the amorphous shell. By crystalline peaks' parameters from Table 3, the nanoparticles size can be calculated by Eq. (7). The nanoparticles' size is of 16.18 nm. The size of nanoparticles determined by this method is more realistic, because it includes a larger number of

particles, and it is not selective as in the case of SEM and AFM.

4. CONCLUSIONS

Polyfurfural was synthesized by a novel, simple and easy method by adding concentrated hydrochloric acid to the monomer solution in ethanol. The polymer was characterized by FT/IR, EDS, and XPS to confirm its structure. The polymer is deposited as globule particles (average size was of 700 nm), which were composed of small spherical particles with average size of about 20.8 nm (by SEM in the synthesis conditions). Polymer thin film was fabricated by anchoring on glass with a rough surface ($Rms = 2.12 \pm 0.3$ nm) and nanoparticles size of 17.8 nm. In x-ray diffraction, the crystallization ratio and the nanocrystals' size (7.42 nm) were calculated. A new method for determining nanoparticle size from x-ray diffraction data is proposed. The particle size was of 16.18 nm that is less than the size specified by SEM or AFM.

5. ACKNOWLEDGEMENT

REFERENCES

1. S. Saravanan, C. Joseph Mathai, M. R. Anantharaman, S. Venkatachalam, D. K. Avasthi, and F. Singh, *Synthetic Metals*, **155**, No. 2: 315 (2005); https://doi.org/10.1016/j.synthmet.2005.09.006

2. S. C. Ng, H. S. O. Chan, P. M. L. Wong, K. L. Tan, and B. T. G. Tan, *Polymer*, **39**, No. 20: 4968 (1998); https://doi.org/10.1016/s0032-3861(97)10029-5

3. B. X. Valderrama-García, E. Rodríguez-Alba, E. G. Morales-Espinoza, K. M. Chane-Ching, and E. Rivera, *Molecules*, **21**, No. 172: 18 (2016); https://doi.org/10.3390/molecules21020172

4. G. H. Shim and S. H. Foulger, *Photonics and Nanostructures — Fundamentals and Applications*, **10**, No. 4: 446 (2012); https://doi.org/10.1016/j.photonics.2011.12.001

5. J. Li, J. Qiao, and K. Lian, *Energy Storage Materials*, **3**, No. 1: 6 (2019); https://doi.org/10.1016/j.ensm.2019.08.012

6. S. C. Hernandez, D. Chaudhuri, W. Chen, N. V. Myung, and A. Mulchandani, *Electroanalysis*, **19**, Nos. 19−20: 2125 (2007); https://doi.org/10.1002/elan.200703933

7. L. Duan, J. Lu, W. Liu, P. Huang, W. Wang, and Z. Liu, *Physicochemical*

and Engineering Aspects, **41,** No. 4: 103 (2012);
https://doi.org/10.1016/j.colsurfa.2012.08.033

8.   H. Gherras, A. Yahiaoui, A. Hachemaoui, A. Belfeda, A. Dehbi, and
       A. I. Mourad, *Journal of Semiconductors*, **39**, No. 9: 102001 (2018);
       https://doi.org/10.1088/1674-4926/39/10/102001

9.   B. S. Dakshayini, K. R. Reddy, A. Mishra, N. P. Shetti, S. J. Malode,
       S. Basu, and A. V. Raghu, *Microchemical Journal*, **2**, No. 61: 1 (2019);
       https://doi.org/10.1016/j.microc.2019.02.061

10.   G. Bayramoğlu, M. Karakışla, B. Altıntaş, A. U. Metin, M. Saçak, and
       M. Y. Arıca, *Process Biochemistry*, **44**, No. 8: 885 (2009);
       https://doi.org/10.1016/j.procbio.2009.04.011

11.   P. M. Carrasco, H. J. Grande, M. Cortazar, J. M. Alberd, J. Areizaga, and
       J. A. Pomposa, *Synthetic Metals*, **156**, Nos. 5−6: 425 (2006);
       https://doi.org/10.1016/j.synthmet.2006.01.005

12.   R. Kumar, S. Singh, and B. C. Yadav, *Iarjset*, **2**, No. 11: 2421 (2015);
       https://doi.org/10.17148/IARJSET.2016.3206

13.   T. Wei, X. Huang, Q. Zeng, and L. Wang, *Journal of Electroanalytical
       Chemistry*, **743**, No. 1: 105 (2015);
       https://doi.org/10.1016/j.jelechem.2015.02.031

14.   Y. Fu, Y. Lin, T. Chen, and L. Wang, *Journal of Electroanalytical Chemistry*, **687**, No. 3: 29 (2012); https://doi.org/10.1016/j.jelechem.2012.09.040

15.   C. J. Mathai, M. Anantharaman, S. Venkitachalam, and S. Jayalekshmi,
       Thin Solid Films, **416**, Nos. 1−2: 15 (2002); https://doi.org/10.1016/s0040-6090(02)00700-9

16.   M. B. Zaman and D. F. Perepichka, *The Royal Society of Chemistry*, **33**,
       No. 1: 4187 (2005); https://doi.org/10.1039/B506138E

17.   D. Ismiyarto, T. Ngadiwiyana, T. Windarti, R. S. Purbowatiningrum,
       M. Hapsari, F. H. Rafi'ah, Suyanti and M. S. Haq, *IOP Conf. Ser.: Materials Science and Engineering*, **172**, No. 1: 012027 (2017);
       https://doi.org/10.1088/1757-899x/172/1/012027

18.   J. Bergström, *Mechanics of Solid Polymers*, **2**, Iss 3: 1 (2015);
       https://doi.org/10.1016/B978-0-323-31150-2.00002-9

19.   L. Yahia and L. K. Mireles, *Characterization of Polymeric Biomaterials*, **5**,
       No. 1: 83 (2017); https://doi.org/10.1016/b978-0-08-100737-2.00004-2

20.   A. Al-Hamdan, A. Al-Falah, and F. Al-Deri, *International Journal of Thin
       Films Science and Technology*, **10**, No. 2: 104 (2021);
       https://doi.org/10.18576/ijtfst/100205

21.   B. Aziz, S. S. Marf, A. Dannoun, E. M. A. Brza, and R. M. Abdullah, *Electrolytes. Polymers*, **12**, No. 10: 2184 (2020);
       https://doi.org/10.3390/polym12102184